Single-molecule magnets based on iron(III) oxo clusters†

Dante Gatteschi,*[a] Roberta Sessoli[a] and Andrea Cornia[b]

[a] *Department of Chemistry, University of Florence, Florence, Italy*
[b] *Department of Chemistry, University of Modena and Reggio Emilia, Modena, Italy. E-mail: gattesch@blu.chim1.unifi.it*

Received (in Cambridge, UK) 14th October 1999, Accepted 15th December 1999
Published on the Web 9th February 2000

Polynuclear compounds of magnetic transition metal ions are attracting large interest after the discovery that their magnetisation may relax very slowly at low temperature. Since their behaviour is similar to that of bulk magnets they may be called single molecule magnets. Here we review the magnetic properties of iron(III) clusters showing such features which may be interesting for future applications, as well as strategies for designing new molecules with increased performances.

Introduction

The magnetic properties of large polynuclear compounds containing transition metal and/or rare earth ions have become the focus of much attention in the last few years,[1–4] after the discovery that the magnetisation of a cluster comprising twelve manganese ions, $[Mn_{12}O_{12}(MeCO_2)_{16}(H_2O)_4]\cdot 2MeCO_2H\cdot 4H_2O$.[5] Mn12Ac, relaxes so slowly at low temperature that the individual molecules behave in manner reminiscent of bulk magnets.[6] In fact if a molecule is magnetised at 2 K by applying a magnetic field, after 2 months the magnetisation is still *ca*. 40% of the saturation value, if the sample is kept at that temperature. In order to achieve the same result at 1.5 K it will be necessary to wait for *ca*. 40 years! Clusters, which behave like Mn12Ac, have been called single-molecule magnets.[1] In a sense this is a misnomer, because the term magnet must rigorously apply only to systems in which the spin correlation length diverges, *i.e.* goes to infinite, and this is clearly not possible in a cluster with a finite size. However the term is evocative, and in our opinion it can be used, provided its true meaning is understood.

One of the features of Mn12Ac which has attracted much interest is that the slow relaxation of the magnetisation gives rise to hysteresis effects, similar to those observed in bulk magnets, but of molecular origin: therefore it becomes in principle possible to store information in one single molecule.[6] The second appealing feature of Mn12Ac is that the relaxation of its magnetisation shows clear quantum effects, and the single molecule magnets can be used to investigate the macroscopic range in which quantum and classical behaviour coexist.[7,8] In principle these features can be exploited for developing new classes of computers in which quantum coherence is used to store and elaborate information. Currently the most promising results seem to be achieved using NMR techniques in solution,[9] but also Josephson junctions and magnetic nanoparticles can be taken into consideration.

In order to be considered for real applications, single molecule magnets must have the highest possible blocking temperature. The blocking temperature is that below which the relaxation of the magnetisation becomes slow compared to the time scale of a particular investigation technique. For instance for NMR the time scale is 10^{-8}–10^{-9} s, while for ac susceptibility measurements it is 10^{-2}–10^{1} s. Therefore the magnetisation of a molecule may appear as blocked in NMR but still dynamic in ac susceptibility measurements. Further it is also important that the molecules show clearly observable quantum effects.

After Mn12Ac, many attempts have been made in order to increase the blocking temperature of the single molecule magnets. In order to reach this goal it is necessary to build molecules which have the largest possible value of the total spin S in the ground state. Mn12Ac itself has $S = 10$ in the ground state, with the magnetisation corresponding to that of an atom with twenty unpaired electrons,[10] but molecules with up to 33 unpaired electrons have been reported.[11] We must emphasize that in general these molecules have many spin states which are thermally populated, therefore the properties associated to the ground state will only show up at low temperatures, when the excited states are depopulated. Clearly in order to increase the blocking temperature it is required that the ground state is the only populated one at relatively large temperatures.

The second requisite for observing single molecule magnet behaviour is that the ground state must have a high magnetic anisotropy of the easy-axis (Ising) type. This means that the magnetisation at low temperature may be stable either parallel or antiparallel to a given axis, and that an energy barrier must be overcome during the reversal of the magnetisation, passing for instance from the orientation 'up' to the orientation 'down'. In

Dante Gatteschi, born in Florence, Italy, in 1945 studied Chemistry at the University of Florence, and he is now Professor of General and Inorganic Chemistry at the same University. His research interests range from the use of spectroscopic techniques, particularly EPR and recently high frequency EPR, for the investigation of metal ion compounds to molecular magnetism. In the latter area his main achievements have been in the field of system comprising metal ions interacting with stable organic radicals and recently in the development of single molecule magnets.

Roberta Sessoli graduated in 1987 and obtained her PhD in Chemistry in 1992 studying the magnetism of molecular materials based on organic stable radicals and transition metal or rare earth ions. Since 1997 she has been an associate researcher at the University of Florence. Her main interests are presently in the magnetism of mesoscopic systems like clusters of magnetic metal ions or nanostructured materials.

Andrea Cornia, born in Modena, Italy, studied Chemistry and graduated in 1992. He obtained his PhD in Chemistry in 1996 under the supervision of D. Gatteschi and A. C. Fabretti. His research interests range from the supramolecular synthesis and structural investigation of nanomagnetic materials to the application of physical techniques in molecular magnetism and solid-state inorganic chemistry.

† Dedicated to the memory of Professor Olivier Kahn.

a system with spin S this occurs when the components with $M = \pm S$ lie lowest ($-S \leq M \leq S$). For axially distorted systems the energies of the M components are given by $E(M) = M^2D$, where D is the axial zero-field splitting (zfs) parameter. Therefore an Ising type anisotropy will be observed when D is negative. For Mn12Ac this condition is met and the barrier for the re-orientation of the magnetisation has been observed to be *ca.* 44 cm^{-1} or 64 K.

Beyond the obvious chemical variants of Mn12Ac,[12–14] other manganese complexes[13,15–17] have been found to behave as single molecule magnets. A few iron,[18–20] chromium[21–23] and vanadium[24] clusters also exhibit similar properties. Certainly the goal of a large ground spin state can be most easily achieved by assembling individual ions with a large ground spin state. Two ions with $S = 5/2$ ferromagnetically coupled have a ground state with $S = 5$, while it is necessary to assemble a cluster of ten $S = 1/2$ ions in order to achieve the same result. This is the reason why ions with large spin, like high spin iron(III) ($S = 5/2$), manganese(III) and iron(II) ($S = 2$), have been largely used.

Iron is certainly a very interesting ion in order to prepare single molecule magnets, not only because of the large spin state, but also because ferritin, the iron-storage protein in most living organisms, can be considered itself as a nanosize magnetic particle. In fact ferritin has been investigated for quantum tunnelling effects of the magnetisation.[25] Many large iron clusters have been reported, ranging from binuclear up to thirty nuclear species. We want to show here how several clusters containing iron behave as single molecule magnets, and discuss which conditions may favour this behaviour. All the clusters of this type so far reported are characterised by antiferromagnetic coupling between the iron(III) ions so that large spin in the ground state can only arise if the number of 'up' spins is different from that of 'down' spins. Therefore the clusters behave as single-molecule ferrimagnets. An example of a bulk ferrimagnet with a similar type of non-compensation of magnetic moments is maghemite, γ-Fe_2O_3. Ferrimagnetic iron–oxo clusters can indeed be considered as models of this prototype mineral.

Properties of iron(III) ions and exchange interactions in pairs

In order to understand which are the best strategies for obtaining single molecule magnets using iron(III) it is necessary to understand which are the conditions favouring both a strong magnetic coupling between the iron ions and a large magnetic anisotropy. The exchange interactions in oxo-bridged iron(III) pairs have been much investigated both theoretically and experimentally, also due to the relevance of these systems to non–heme metallo-proteins containing binuclear iron units in their active site.[26,27] The simplest approach considers two parameters, the average metal–oxygen distance, P, and the metal–oxygen–metal angle, α. Magnetic data recorded on a large series of iron complexes suggest that the P-dependence of the exchange coupling constant, J, is well represented by eqn. (1):[27]

$$J = 1.753 \times 10^{12} \exp(-12.663P) \quad (1)$$

where J is expressed in cm^{-1}, P in Å, and the exchange Hamiltonian is in the form $H = JS_1 \cdot S_2$. The coupling constant is largely insensitive to the Fe–O–Fe angle for $\alpha > 120°$. For smaller angles an effect is clearly observed, J becoming smaller as the angle α is reduced. A systematic study has been performed in a series of binuclear complexes with two alkoxo bridges[28] and similar Fe–O distances. The values of α range from 102 to 106°, while J varies between *ca.* 15 and 21 cm^{-1}. The simplest correlation was found to be of the type given by eqn. (2):

$$J = 1.48\,\alpha - 135 \quad (2)$$

with J in cm^{-1} and α in degrees. An extrapolation of eqn. (2) suggests that for $\alpha \approx 90°$ the coupling should become ferromagnetic. A justification for these experimental results was found on the basis of extended Hückel calculations, which however indicate that for small angles ($\alpha \approx 90°$) the coupling should become antiferromagnetic again, due to the importance of direct overlap between the iron(III) magnetic orbitals. In fact if the Fe–O bond distances are kept constant while the α angle is progressively reduced, the shortening of the Fe–Fe distance favours direct exchange. More experimental data are certainly needed to check this prediction. It should be remarked that the decrease in the antiferromagnetic coupling constant for a < 120° has been predicted also by a complete exchange model recently suggested by Güdel and Weihe.[29]

The anisotropy of the pairs depends on the anisotropy of the individual ions, and on an additional term that is brought about by the interaction between the two iron ions.[30] The former contribution is referred to as single-ion anisotropy, while the latter is known as spin–spin anisotropy. High spin iron(III) has a d^5 configuration, which yields an orbital singlet ^6S ground term for the free ion. The ground state of the complexed ion is also orbitally non-degenerate, therefore the Zeeman anisotropy is very low, with $g_x \approx g_y \approx g_z \approx 2.0023$. However some admixture with excited states of lower spin multiplicity is allowed by spin–orbit coupling and the ground $S = 5/2$ state does show zero field splitting, which may easily be of the order of 1 cm^{-1}. This splitting determines the single ion anisotropy.

Single ion contributions to the anisotropy cannot be rigorously calculated, and so far even the experimental data are lacking in the sense that no significant correlation between structural features and values of D has been established. Recently Neese and Solomon have suggested[31] that it is possible to calculate the zfs parameters by using a MO approach, while traditional ligand field models have been implemented in the Angular Overlap Model, AOM, formalism.[32] For instance it has been found that a trigonal distortion from octahedral geometry yields a negative zfs parameter D for elongation, and positive for compression. In order to have direct information on the zfs in model compounds the HF-EPR spectra of a tris ß-diketonate complex, $Fe(dpm)_3$, where dpm = 2,2,6,6-tetramethylheptane-3,5-dionate, were recorded.[20] The spectra yielded $D = -0.18\ cm^{-1}$ and $E/D = 0.25$. These values were reproduced in a reasonable way by using the AOM. However, more experimental and theoretical work is needed in order to establish useful correlations between structure and zfs of iron(III) ions. Given their relevance also for biological systems this seems to be indeed an important task.

The anisotropy associated with the spin–spin interaction can be described to a good approximation by the interaction between the magnetic point dipoles centred on the two iron ions. For a pair of antiferromagnetically coupled ions the dipolar interaction orients the two spins orthogonal to the vector $\boldsymbol{r}$ connecting the two centres. In fact the poles of the same sign would be in contact for an orientation parallel to $\boldsymbol{r}$. Therefore the plane perpendicular to $\boldsymbol{r}$ [Fig. 1(a)] is a hard plane for the magnetisation of the antiferromagnetic dimer, which is more easily magnetised when the field is applied parallel to the axis connecting the two spins. Dipolar interactions thus provide an Ising-type contribution to the magnetic anisotropy.

These considerations can be extended to polynuclear systems as well. In particular, when antiferromagnetically coupled metal ions are arranged in a planar structure with axial symmetry, like in some of the iron(III) clusters described in the forthcoming sections, nearest-neighbour dipolar interactions determine a *XY*-anisotropy with an easy plane of magnetisation when the ground state has $S = 0$ [Fig. 1(b)]. In fact, in the lowest-energy configuration, the individual spins are antiparallel to their nearest neighbours (owing to exchange interactions) *and* perpendicular to the average plane through the metal array

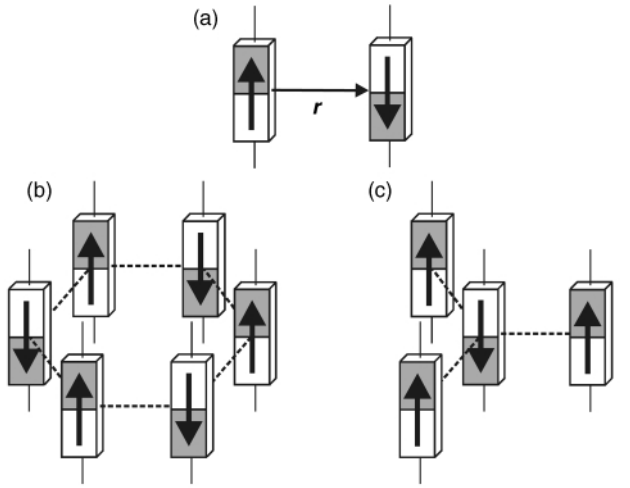

Fig. 1 Schematic view of the preferred spin orientation due to the dipolar interaction in an antiferromagnetic dimer (a), in a cyclic antiferromagnetic cluster (b), and in a ferrimagnetic tetrameric cluster (c).

(owing to dipolar interactions). By contrast, when the ground state has *S* different from zero, *i.e.* in ferrimagnetic clusters, the system exhibits an Ising-type anisotropy [Fig. 1(c)]. It is noteworthy that dipolar interactions alone lead to an Ising-type anisotropy in planar ferrimagnetic clusters, thus giving the possibility to observe single molecule magnet behaviour. The topology of the metal ions can thus strongly influence magnetic anisotropy *via* dipole–dipole interactions, establishing a direct connection between the shape of the cluster and its magnetic properties.

Iron rings: quantum size effects and anisotropy

Using alkoxides or carboxylates as bridging ligands it has been possible to synthesise six-,[33,34] eight, ten-[35] and twelve-[36] membered iron(III) rings. In all the cases the iron–iron interaction is antiferromagnetic, yielding a ground $S = 0$ state. The energies of the lowest lying *S* states can be expressed by eqn. (3):

$$E(S) = J_{\text{eff}}S(S + 1) \qquad (3)$$

where $J_{\text{eff}} = 4J/N$, with *N* the number of iron ions in the ring. Below 1 K the rings are in the non-magnetic ground state, and consequently under low field conditions the magnetisation is zero. However, on increasing the field, the excited magnetic states are stabilised, until eventually they become the ground state. This gives rise to a typical stepped magnetisation, with a first jump at the field where the lowest lying $S = 1$ state becomes the ground state, then where the $S = 2$ crosses over to become the ground state, and so on.[35,37] These observations are clear evidence for quantum effects, corresponding to the fact that the lowest $S = 0$ level is separated by a gap from the first excited level. The larger the ring the smaller the gap, until eventually the levels must merge in a continuum. In fact the magnetisation of one-dimensional magnetic materials, that can be considered as the extrapolation of rings to infinite, does not show steps.[38] Therefore it would be extremely important to make available larger and larger rings in order to follow the passage from microscopic to bulk. In fact the thermodynamic properties calculated for finite rings have long been used to extrapolate the properties of the infinite chains. Another interesting goal is that of synthesising odd membered rings of half integer spins, which should show spin frustration effects.[39]

All the measurements referred to above are static measurements, which do not provide any information on the dynamics of the magnetisation and on possible tunnelling phenomena. Dynamic measurements can in principle be made with a variety of techniques, ranging from ac susceptometry to magnetic resonance. In this respect NMR is particularly appealing, because it can monitor the variations in the relaxation rate of the nuclear moments under the influence of the electron magnetisation. In fact, it can be expected that when two levels cross, the electron relaxation at low temperature is drastically influenced. Therefore the field dependence of the nuclear relaxation rate should show anomalies corresponding to the crossover fields. This has been recently observed[40] in a decanuclear ring, the so-called ferric wheel, whose structure is shown in Fig. 2. All the methods exploiting NMR have potential interest for quantum computing applications, given the recent implementation of NMR techniques in solution.[9]

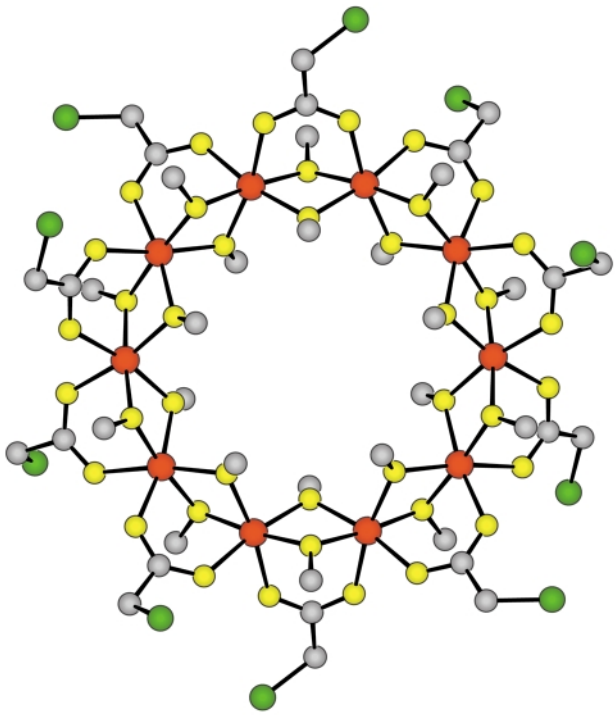

Fig. 2 View of the structure of the cluster $[Fe(OMe)_2(O_2CCH_2Cl)]_{10}$, the so-called 'ferric wheel'. The iron atoms are in red, oxygen in yellow, carbon in grey and chlorine in green. The ten iron atoms lie in a plane within ±0.009 Å and the diameter of the cluster, defined as the longest Fe···Fe distance, is 9.80 Å.

Stepped magnetisation has been observed also in smaller iron(III) rings, like LiFe6 and NaFe6, whose structure is depicted in Fig. 3 The alkali-metal ion, Li^+ or Na^+, is hosted in the. centre of the ring, which behaves like an inorganic crown ether.[34] Solution studies have shown that the affinity of the Fe6 ring is higher for sodium than for lithium ions. Further, LiFe6 and NaFe6 can be neatly obtained by adding lithium or sodium ions to a solution of a twelve-membered iron(III) ring which does not host any alkali-metal ion.[36]

The magnetisation of small single crystals of LiFe6 and NaFe6 was investigated through new torque magnetometers using a sensitive cantilever which directly provided the magnetic anisotropy of the excited *S* states.[41] The central alkali-metal ion strongly influences not only the isotropic exchange interaction, which passes from 14 to 20 cm^{-1} by replacing Li^+ with Na^+, but also the magnetic anisotropy. In fact the zero-field splitting of the first excited $S = 1$ state is $D = 1.16$ cm^{-1} for the lithium derivative and $D = 4.32$ cm^{-1} for the sodium derivative. The former value corresponds almost exactly to the calculated dipolar contribution. By contrast, the magnetic anisotropy of the sodium derivative points to the presence of large single ion contributions. Minor differences in the environment of the individual iron(III) centers, such as those induced by the different size of the guest ion, may thus induce

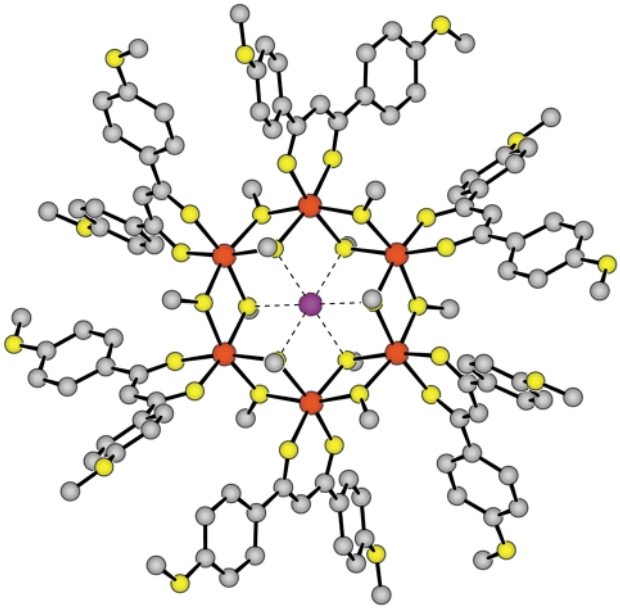

Fig. 3 View of the structure of the hexanuclear iron cluster $[NaFe_6(OMe)_{12}(pmdbm)_6]^+$, where pmdbm = 1,3-di(4-methoxyphenylpropane)-1,3-dionate (colour code as in Fig. 2). Li^+ can replace the Na^+ cation in the centre with significant changes in the intracluster magnetic exchange interaction and in the magnetic anisotropy.

large zfs variations. This clearly indicates that the control of the magnetic anisotropy of the clusters is a difficult task.

Iron-containing single molecule magnets

The smallest iron cluster showing slow relaxation effects in the magnetisation at low temperature is $[Fe_4(OMe)_6(dpm)_6]$, Fe4.[20] The structure of Fe4 is shown in Fig. 4. A central iron ion is

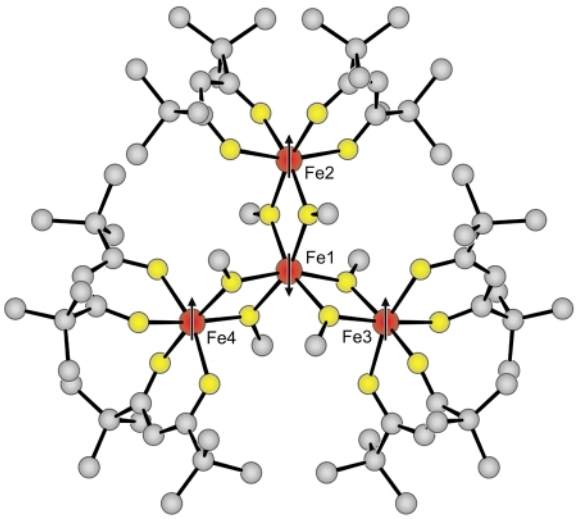

Fig. 4 Structure of the ferrimagnetic cluster $[Fe_4(OMe)_6(dpm)_6]$ where dpm = 2,2,6,6-tetramethylheptane-3,5-dionate (colour code as in Fig. 2). The arrows correspond to the spin structure in the ground $S = 5$ state.

connected to three terminal ions by three double μ-alkoxo bridges. Crystal symmetry requires a C_2 axis in the cluster passing through Fe1 and Fe2. The three external iron(III) ions define an almost equilateral triangle. In this case the spin topology, which for antiferromagnetic coupling orients the central spin 'down' and the external ones 'up' determines the non-compensation of the spins. The ground state has $S = 5$, and the ferrimagnetic nature of the cluster is clearly shown by the χT *vs.* T curve which goes through a broad minimum at *ca.* 150 K and then reaches 14.6 emu K mol^{-1} at low temperature, in reasonable agreement with an $S = 5$ state ($\chi T = 15$ emu K mol^{-1}, for $g = 2.00$). The temperature dependence of χT has been successfully reproduced calculating the energies of the total spin states using the spin Hamiltonian eqn. (4):

$$H = J\,(\boldsymbol{S_1}\bullet\boldsymbol{S_2} + \boldsymbol{S_1}\bullet\boldsymbol{S_3} + \boldsymbol{S_1}\bullet\boldsymbol{S_4}) + J'\,(\boldsymbol{S_2}\bullet\boldsymbol{S_3} + \boldsymbol{S_3}\bullet\boldsymbol{S_4} + \boldsymbol{S_2}\bullet\boldsymbol{S_4}) \quad (4)$$

The best-fit values are: $J = 21.1$ cm^{-1}, $J' = -2.1$ cm^{-1}, in reasonable agreement with the values expected using eqns. (1) and (2).

The anisotropy of the ground state has been determined using high field EPR spectroscopy, and it has been shown to be quasi axial, and of the Ising type, with $D = -0.20$ cm^{-1}. This means that the ground $S = 5$ state is split in such a way that the $M = \pm5$ levels lie lowest, with $M = \pm 4$ at 1.8 cm^{-1}, $M = \pm3$ at 3.2 cm^{-1}, $M = \pm2$ at 4.2 cm^{-1} and $M = 0$ at 5 cm^{-1}. If the system is magnetised at low temperature, the $M = -S$ state will be selectively populated. On switching the field off, the system will revert to thermal equilibrium, *i.e.* it will equalise the populations of the $M = -S$ and $M = +S$ states. At the simplest level of approximation this cannot occur directly, but the system must climb all the levels, one at a time, up to $M = 0$, and then descend.[42] Under this simplifying approximation the barrier for the re-orientation of the magnetisation is given by the difference in energy between the lowest $M = +S$ and the top $M = 0$ level [eqn. (5)]:

$$\Delta = |D|\,S^2 \quad (5)$$

and the relaxation of the magnetisation is expected to follow the Arrhenius law:

$$\tau = \tau_0 \exp(\Delta/kT) \quad (6)$$

where τ_0 is expected to be proportional to S^6/Δ^3. Eqn. (6) is the same as that appropriate to classical superparamagnets.[43]

Below 1 K Fe4 shows slow relaxation of the magnetisation in ac susceptibility measurements. The relaxation time follows the Arrhenius law with $\tau_0 = 1.1 \times 10^{-6}$ s and $\Delta/k = 3.5$ K. This means that at 0.2 K, the lowest measurement temperature, the relaxation time is of the order of one minute. This relaxation is much faster than that of Mn12Ac,[6] as it should be expected given the smaller S and the lower barrier.

The height of the barrier, calculated with eqn. (5), is larger than the experimental value. This has been found to be the case in all systems showing slow relaxation of the magnetisation investigated so far. It must be concluded that eqn. (5) is only a loose approximation. In particular, the simplified model does not take into account direct tunnelling within a formally degenerate $\pm M$ pair. This point will be addressed in detail in the following section on Fe8.

Given the small number of magnetic ions in Fe4, detailed calculations were performed of the energies of the spin levels. Attempts were made also to rationalise the anisotropy of the ground state. As outlined in a previous section, the dipolar contribution has the same sign as the observed anisotropy, although spin–spin interactions alone can not quantitatively account for it. Attempts were made to calculate the single ion contributions, using the AOM, but no really acceptable results were achieved.[20] More efforts are needed in this field.

Fe8, the quantum magnet

The structure of $[Fe_8O_2(OH)_{12}(tacn)_6]^{8+}$, Fe8, where tacn = 1,4,7-triazacyclononane, which Wieghardt *et al.* originally reported as the bromide salt,[44] Fe8Br, is shown in Fig. 5. The analysis of the temperature dependence of the magnetic susceptibility,[45] provided evidence for a ground $S = 10$ state, which can occur if six spins are up and two down. Since there are several triangles in the exchange pathways connecting the iron(III) ions spin, frustration effects[39] can be anticipated. This means that the ground state is not correctly described by simply putting the spins up or down on different metal ions. However

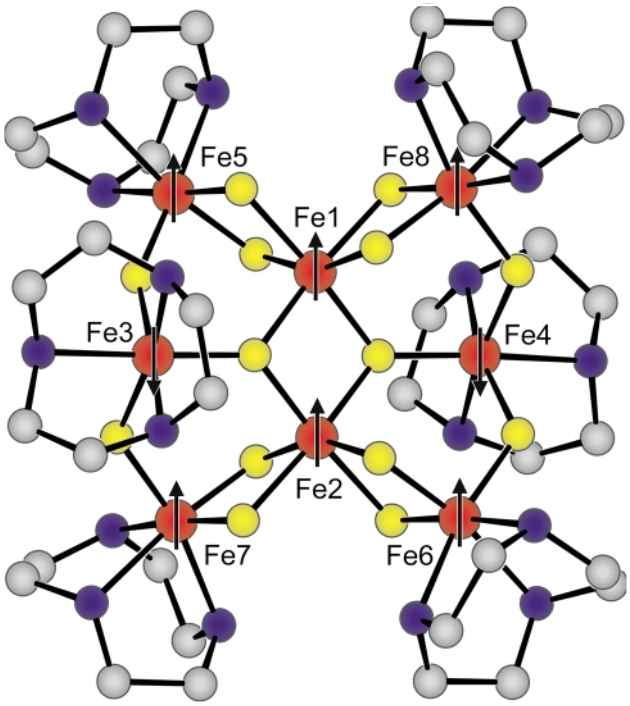

Fig. 5 View of the cluster $[Fe_8O_2(OH)_{12}(tacn)_6]^{8+}$ where tacn = 1,4,7-triazacyclononane. The arrows correspond to the spin structure previously suggested by the analysis of the magnetic susceptibility and then determined from single crystal polarised neutron diffraction experiments (see ref. 46).

it was possible to obtain a direct picture of the spin density by using polarised neutron diffraction techniques.[46] These showed that the spin density on Fe3 and Fe4 is negative, and that on all the other iron ions is positive. These data are in qualitative agreement with the values obtained from the fit of the temperature dependence of the magnetic susceptibility. The spin density however does not correspond to five unpaired electrons on each iron ion, confirming that the 'up-down' description is an oversimplification.

The ground state is largely split in zero field, as evidenced by HF-EPR[19] and inelastic neutron scattering, INS,[47] experiments. When neutrons interact with the clusters they may induce transitions between the M levels of S multiplets, according to the selection rules $\Delta M = 0, \pm 1$. Therefore, by measuring the INS it is possible to obtain detailed information on the spectrum of the M energy levels. The INS of Fe8Br is particularly rich, and it has shown, for the first time, how the technique can be fruitfully used also on systems with many protons in the energy window up to 60 cm^{-1}. In fact, after the spectra of Fe8Bt, recently the spectra of Mn12Ac have been reported[48] showing a similar abundance of absorptions. The INS spectra of Fe8Br are shown in Fig. 6, together with the assignment of the peaks to the transitions within the lowest $S = 10$ multiplet.

The HF-EPR and the INS spectra have provided essentially the same sets of parameters to describe the splitting of the ground $S = 10$ state. In particular, they agree on the fact that the spin Hamiltonian for describing the zero field splitting requires the inclusion of both second order and fourth order terms. This means that the splitting of the ground state is determined by both quadrupolar terms, described by the parameters D and E, and hexadecupolar terms described by the B_4^0, B_4^2 and B_4^4 parameters. Single crystal EPR spectra have also provided the principal directions of the zero field splitting tensors, and consequently the principal directions of the magnetic anisotropy. The easy axis, *i.e.* that of prevailing orientation of the individual spins, makes a small angle, *ca.* 10°, with the perpendicular of the plane of the iron ions, while the hard axis

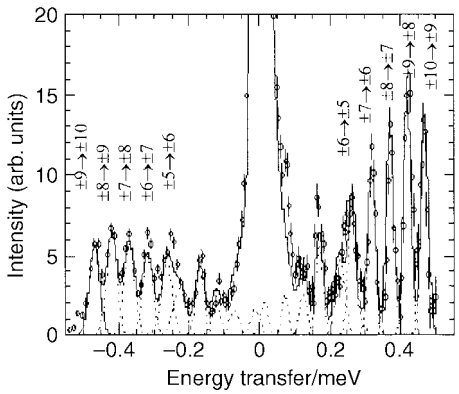

Fig. 6 Inelastic neutron scattering spectrum recorded at 10 K on Fe8Br cluster microcrystalline powder. The large peak at zero energy corresponds to the elastic contribution. On the left side the emission spectrum is reported while on the right side are the absorption lines. The transitions at the extremes of the spectrum can be easily assigned as shown in the picture using the basis of the eigenvalues of $\boldsymbol{S}_z$ (1 meV = 8.065 cm^{-1}).

passes through the Fe1 and Fe2 ions. The energies of the M levels of Fe8Br are shown in Fig. 7. The lowest lying levels

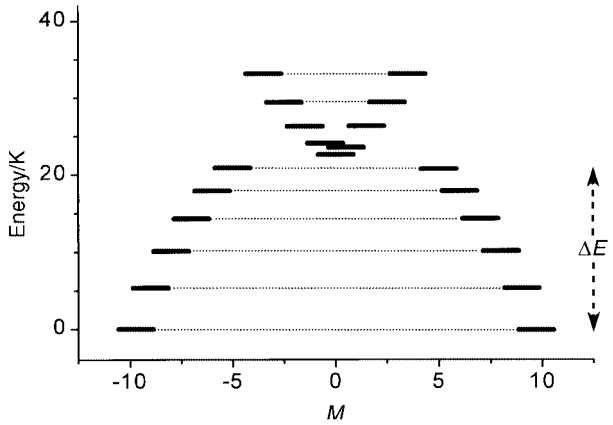

Fig. 7 Schematic view of the splitting in zero field of the $S = 10$ ground manifold of Fe8Br using the spin Hamiltonian parameters of ref. 47. The height of the classical energy barrier is shown. Underbarrier transitions dominate at low temperature. The levels above *ca.* 22 K cannot be labelled with M and their assignment on the graph is arbitrary.

correspond to $M = \pm S$, and on increasing temperature, the levels are progressively more admixed. This is essentially determined by the non-zero E parameter that admixes levels differing in M by ±2. In particular from Fig. 7 we learn that at the top of the manifold there is not a unique level corresponding to $M = 0$. Therefore the meaning of eqn. (5) for defining the barrier for the reorientation of the magnetisation is completely lost and the barrier is significantly reduced.[49] However, if it is used in a first approximation, Δ/k is calculated to be 29 K, and therefore slow relaxation effects are expected at low temperature.

In Mössbauer experiments, which have a time scale of 10^{-8}–10^{-9} s slow relaxation of the magnetisation of Fe8Br is observed[19] below 20 K, while the same effect can be detected by ac susceptibility measurements only below 3 K. The relaxation times however do not rigorously obey an Arrhenius type relation (6). The relaxation time of the magnetisation becomes so slow below 1 K that hysteresis loops of molecular origin can be observed.[50] The hysteresis, shown in Fig. 8, has a dynamic nature, as revealed by the strong dependence on the rate of the field sweep, and the same stepped appearance first reported for Mn12Ac.[7,8] The flat regions correspond to fields at which the relaxation is slow, while the steps correspond to fields at which a rapid increase of the relaxation rate is observed. This behaviour has been attributed to thermally assisted quantum tunnelling. In a magnetic quantum system the relaxation of the magnetisation may occur either with the mechanism described

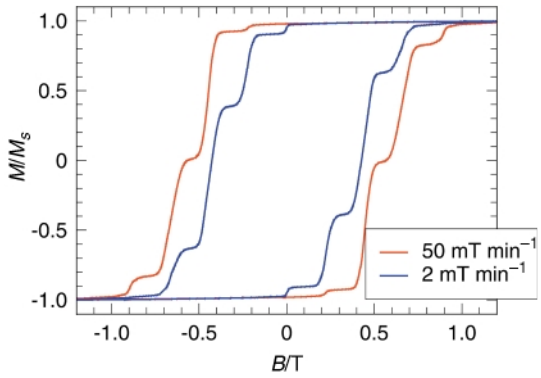

Fig. 8 Hysteresis loops recorded for Fe8Br at 0.30 K and two different field scan speeds. The dynamic nature of the hysteresis is revealed by the strong dependence on the sweep rate. The stepped shape is due to the tunnelling of the magnetisation, which occurs when two levels on the opposite sides of the barrier are brought in coincidence by sweeping the field, which accelerates the magnetic relaxation giving rise to the jumps in the magnetisation.

above, where the absorption or emission of a phonon allow the transition from the M to the $M \pm 1$ level, or by tunnelling between pairs of degenerate levels. In zero field the lowest lying pairs of M levels meet the tunnelling condition, and the relaxation is comparatively fast. In the presence of an external field the energy of the $+M$ level increases and that of the $-M$ level decreases, making quantum tunnelling impossible, as shown schematically in Fig. 9. However the condition for

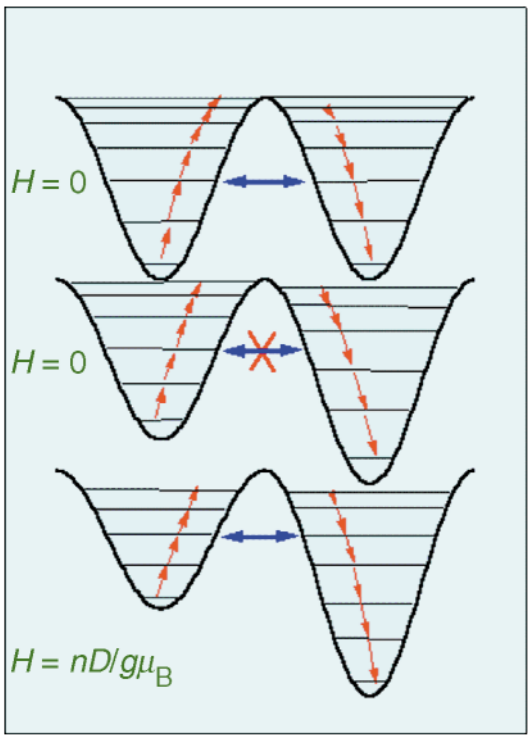

Fig. 9 Schematic drawing of the energy barrier for the reversal of the magnetisation generated by the magnetic anisotropy. The levels correspond to the M states of the ground spin multiplet and for the sake of clarity an axial zero field splitting has been considered. In zero applied field the $\pm M$ states are degenerate allowing a shortcut of the barrier through a tunnelling process. An external magnetic field removes the energy correspondence of the states on the opposite sides of the barrier, thus hampering the underbarrier mechanism of relaxation, except for critical values of the field for which the energy correspondence is re-established.

tunnelling are restored for fields at which the $+M$ level has the same energy as of the $-M + n$ level, where $n = 1,2,\ldots$*etc*. The fields where these conditions are met can be calculated using the spin Hamiltonian parameters obtained from HF-EPR and INS experiments. The calculated fields correspond to the fields where steps are observed in the hysteresis. These tunnelling processes occur not only between the lowest levels, but also between the higher thermally populated levels. Therefore the overall mechanism has been described as thermally assisted quantum tunnelling.

Direct measurements of the relaxation time of Fe8Br can be performed at low temperature by first saturating the magnetisation and then monitoring its time decay.[50] In this way it is observed that below 350 mK the relaxation becomes temperature independent, thus confirming the quantum tunnelling effects. Under these conditions only the lowest $M = 10$ levels are populated, and tunnelling occurs between them. This has been the first experimental evidence of pure quantum tunnelling in a magnetic nanoparticle. Attempts to observe this behaviour in particles obtained by techniques other than molecular chemistry had failed, essentially because it was impossible to have absolutely monodisperse particles.

The way the molecules undergo tunnelling is still a matter of debate, but evidence is accumulating in favour of the mechanism to be discussed below. The $M = \pm 10$ levels are degenerate in axial symmetry. If a transverse anisotropy is present, *i.e.* a matrix element different from zero, $\Delta/2$, connects the two states, then tunnelling is possible. The two levels are split by the transverse field, $H_t = \Delta/g\mu_B$, and the magnetisation can fluctuate with a frequency proportional to Δ, the tunnel splitting. This picture is correct if no additional fields are present. These however cannot be avoided because the molecule is embedded in a lattice with other magnetised molecules that generate a dipolar field, H_d. If this is larger than H_t the effect of the matrix element is quenched and no tunnelling is observed. In Fe8Br, H_d is of the order of 1–10 mT, while H_t is of the order of 10^{-9} T, therefore the condition for tunnelling is not met at this level of approximation. However the above picture neglects the role of the magnetic nuclei present in the cluster. The ^{1}H ($I = 1/2$), ^{14}N ($I = 1$), and ^{79,81}Br ($I = 3/2$) nuclei generate a fluctuating hyperfine field, H_{hy}, at the magnetic centres broadening the $M = \pm 10$ levels. The broadening is of the order of 1 mT and it may restore the tunnelling conditions for the molecules for which $H_d < H_{hy}$. However, since the distribution of dipolar fields is broader than that of hyperfine fields, the process should stop soon. In order to justify the observed continuous quantum relaxation to thermal equilibrium it must be considered that when a molecule tunnels it changes its magnetisation. Consequently, the dipolar field felt by the neighbouring molecules also changes, creating regions in the sample where the condition $H_d < H_{hy}$ is met.

Another way of imposing the condition that the tunnel splitting is larger than the local fields is to apply a field perpendicular to the easy axis. The applied field will increase the tunnel splitting which then can be more easily measured.

Using micro SQUID techniques it was also possible to measure the intrinsic width of the tunnel splitting.[51] This has been experimentally shown to be proportional to the hyperfine field in Fe8Br.[52] In fact when the naturally occurring non-magnetic Fe isotopes have been substituted with the magnetic ^{57}Fe ($I = 1/2$) the width of the splitting has been measured to increase from 0.8 to 1.2 mT as shown in the inset of Fig. 10. When the ^{1}H nuclei are partially substituted with the less magnetic ^{2}H nuclei the width decreased to 0.6 mT. The hyperfine field generated by the nuclei also strongly affects the relaxation rate of the macroscopic magnetisation, which is fastest in ^{57}Fe-enriched samples and slowest in the partially deuterated ones. This is shown in Fig. 10, where the time needed to relax 1% of the saturation magnetisation is plotted as a function of the temperature. These results showed the fundamental role of nuclei for the relaxation of the magnetisation of Fe8Br in the quantum regime and open the possibly of controlling the dynamics of the magnetisation by acting on the nuclei.

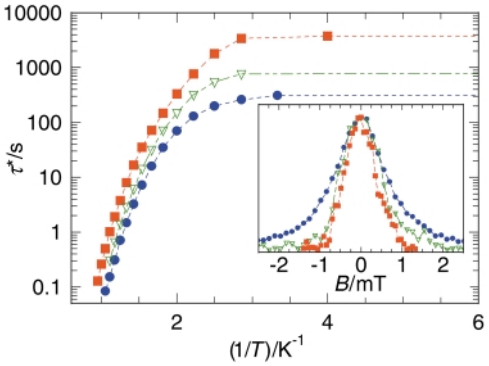

Fig. 10 Isotopic effect on the relaxation of the magnetisation and on the intrinsic line-width of the resonant tunnelling process (inset). τ^* corresponds to the time needed to relax 1% of the saturation magnetisation and its temperature dependence is studied for three isotopic samples of Fe8Br: natural sample (green),^{57}Fe enriched sample (blue), partially deuterated sample (red). In the inset the resonance line, estimated from the field dependence of the relaxation rate, is reported for the three isotopic samples. In order to study the intrinsic linewidth and to avoid the broadening due to dipolar interaction a hole-burning technique has been employed (see ref. 51).

Chemical modifications to Fe8Br have been also attempted. So far the most successful has been the partial substitution of bromide anions with perchlorate anions. $[Fe_8O_2(OH)_{12}(tacn)_6]Br_4(ClO_4)_4$, Fe8ClO4, has been shown to behave similarly to Fe8Br, with a ground $S = 10$ state. However the zfs of the ground state is slightly different in the two compounds. In particular the E/D ratio, which determines the rhombic splitting of the magnetic anisotropy, is larger than that of Fe8Br. Therefore the blocking temperature and the onset of quantum regime are different. It may be hoped that these small variations may provide additional handles to test the theories of quantum tunnelling.

Perspectives

The field of molecular nanomagnetism is just at the beginning. The advantage of molecular clusters, compared to all the other types of magnetic nanoparticles, is that they are all identical to each other and their structure is known. Further, intermolecular interactions in the crystal lattice are so weak that in most cases the response of the crystal is the same as that of an individual molecule. Therefore it is possible to measure a molecular response by using traditional macroscopic techniques. On the other hand, the fact that the molecules are bistable makes them interesting objects to be addressed individually. Therefore it can be foreseen that in the next few years techniques to address single molecules will be developed. Another important development to be expected is the synthesis of larger clusters, which will be investigated for a large number of different properties, such as those related with biocompatibility (for MRI contrast agents, or for magnetic drug delivery) and for the development of new physics. In fact the results already obtained have shown that these materials open exciting new perspectives in mesoscopic physics. For instance Fe8Br has for the first time provided an experimental confirmation of the so-called Berry phase in magnets,[53] a phenomenon long looked for. There are high expectations for the fundamental contributions that this highly interdisciplinary area can bring.

Acknowledgements

The financial support of MURST, CNR and PFMSTAII is gratefully acknowledged. We gratefully acknowledge G. Amoretti, R. Caciuffo, A. Caneschi and W. Wernsdorfer.

Notes and references

1 G. Aromi, S. M. J. Aubin, M. A. Bolcar, G. Christou, H. J. Eppley, K. Folting, D. N. Hendrickson, J. C. Huffman, R. C. Squire, H. L. Tsai, S. Wang and M. W. Wemple, *Polyhedron*, 1998, **17**, 3005.
2 B. Barbara, L. Thomas, F. Lionti, A. Sulpice and A. Caneschi, *J. Magn. Magn. Mater.*, 1998, **177**, 1324.
3 D. Gatteschi, A. Caneschi, L. Pardi and R. Sessoli, *Science*, 1994, **265**, 1054.
4 A. Muller, F. Peters, M. T. Pope and D. Gatteschi, *Chem. Rev.*, 1998, **98**, 239.
5 A. Caneschi, D. Gatteschi, R. Sessoli, A.-L. Barra, L. C. Brunel and M. Guillot, *J. Am. Chem. Soc.*, 1991, **113**, 5873.
6 R. Sessoli, D. Gatteschi, A. Caneschi and M. A. Novak, *Nature (London)*, 1993, **365**, 141.
7 L. Thomas, F. Lionti, R. Ballou, D. Gatteschi, R. Sessoli and B. Barbara, *Nature (London)*, 1996, **383**, 145.
8 J. R. Friedman, M. P. Sarachik, J. Tejada and R. Ziolo, *Phys. Rev. Lett.*, 1996, **76**, 3830.
9 I. L. Chuang, N. Gershenfeld and M. Kubinec, *Phys. Rev. Lett.*, 1998, **80**, 3408.
10 R. Sessoli, H. L. Tsai, A. R. Schake, S. Wang, J. B. Vincent, K. Folting, D. Gatteschi, G. Christou and D. N. Hendrickson, *J. Am. Chem. Soc.*, 1993, **115**, 1804.
11 A. K. Powell, S. L. Heath, D. Gatteschi, L. Pardi, R. Sessoli, G. Spina, F. Del Giallo and F. Pieralli, *J. Am. Chem. Soc.*, 1995, **117**, 2491.
12 Z. M. Sun, D. Ruiz, E. Rumberger, C. D. Incarvito, K. Folting, A. L. Rheingold, G. Christou and D. N. Hendrickson, *Inorg. Chem.*, 1998, **37**, 4758.
13 S. M. J. Aubin, S. Spagna, H. J. Eppley, R. E. Sager, G. Christou and D. N. Hendrickson, *Chem. Commun.*, 1998, 803.
14 Z. M. Sun, C. M. Grant, S. L. Castro, D. N. Hendrickson and G. Christou, *Chem. Commun.*, 1998, 721.
15 E. K. Brechin, J. Yoo, M. Nakano, J. C. Huffman, D. N. Hendrickson and G. Christou, *Chem. Commun.*, 1999, 783.
16 B. Pilawa, M. T. Kelemen, S. Wanka, A. Geisselmann and A. L. Barra, *Europhys. Lett.*, 1998, **43**, 7.
17 A. L. Barra, A. Caneschi, D. Gatteschi, D. P. Goldberg and R. Sessoli, *J. Solid State Chem.*, 1999, **145**, 484.
18 K. L. Taft, G. C. Papaefthymiou and S. J. Lippard, *Science*, 1993, **259**, 1302.
19 A. L. Barra, P. Debrunner, D. Gatteschi, Ch. E. Schulz and R. Sessoli, *Europhys. Lett.*, 1996, **35**, 133.
20 A. L. Barra, A. Caneschi, A. Cornia, F. Fabrizi de Biani, D. Gatteschi, C. Sangregorio, R. Sessoli and L. Sorace, *J. Am. Chem. Soc.*, 1999, **121**, 5302.
21 S. Ferlay, T. Mallah, R. Ouahes, P. Veillet and M. Verdaguer, *Inorg. Chem.*, 1999, **38**, 229.
22 T. Mallah, C. Auberger, M. Verdaguer and P. Veillet, *J. Chem. Soc., Chem. Commun.*, 1995, 61.
23 A. Scuiller, T. Mallah, M. Verdaguer, A. Nivorozkhin et al., *New J. Chem.*, 1996, **20**, 1.
24 S. L. Castro, Z. M. Sun, C. M. Grant, J. C. Bollinger, D. N. Hendrickson and G. Christou, *J. Am. Chem. Soc.*, 1998, **120**, 2365.
25 E. M. Chudnovsky, *J. Magn. Magn. Mater.*, 1998, **185**, 267.
26 D. M. Kurtz, *Chem. Rev.*, 1990, **90**, 585.
27 S. M. Gorun and S. J. Lippard, *Inorg. Chem.*, 1991, **30**, 1625.
28 F. Le Gall, F. Fabrizi de Biani, A. Caneschi, P. Cinelli, A. Cornia, A. C. Fabretti and D. Gatteschi, *Inorg. Chim. Acta*, 1997, **262**,123.
29 H. Güdel and H. U. Weihe, *J. Am. Chem. Soc.*, 1998, **120**, 2870.
30 A. Bencini and D. Gatteschi, *EPR of Exchange Coupled Systems*, Springer-Verlag, Berlin, 1990.
31 F. Neese and E. I. Solomon, *Inorg. Chem.*, 1998, **37**, 6568.
32 A. Bencini, I. Ciofini and M. G. Uytterhoeven, *Inorg. Chim. Acta*, 1998, **274**, 90.
33 R. W. Saalfrank, I. Bernt, E. Uller and F. Hampel, *Angew. Chem., Int. Ed. Engl.*, 1997, **36**, 2482.
34 A. Caneschi, A. Cornia and S. J. Lippard, *Angew. Chem., Int. Ed. Engl.*, 1995, **34**, 467.
35 K. L. Taft, C. D. Delfs, G. C. Papaefthymiou, S. Foner, D. Gatteschi and S. J. Lippard, *J. Am. Chem. Soc.*, 1994, **116**, 823.
36 A. Caneschi, A. Cornia, A. C. Fabretti and D. Gatteschi, *Angew. Chem., Int. Ed.*, 1999, **38**, 1295.
37 A. Caneschi, A. Cornia, A. C. Fabretti, S. Foner, D. Gatteschi, R. Grandi and L. Schenetti, *Chem. Eur. J.*, 1996, **2**, 1379.
38 J. Sinzig, L. J. De Jongh, A. Ceriotti, R. Della Pergola, G. Longoni, M. Stener, K. Albert and N. Rosch, *Phys. Rev. Lett.*, 1998, **81**, 3211.
39 C. A. Christmas, H. L. Tsai, L. Pardi, J. M. Kesselman, P. K. Gantzel, R. K. Chadha, D. Gatteschi, D. F. Harvey and D. N. Hendrickson, *J. Am. Chem. Soc.*, 1993, **115**, 12483.

40 M. H. Julien, Z. H. Jang, A. Lascialfari, F. Borsa, M. Horvatic, A. Caneschi and D. Gatteschi, *Phys. Rev. Lett.*, 1999, **83**, 227.
41 A. Cornia, M. Affronte, A. G. M. Jansen, G. L. Abbati and D. Gatteschi, *Angew. Chem., Int. Ed.*, 1999, **38**, 2264.
42 F. Hartmann-Boutron, P. Politi and J. Villain, *Int. J. Mod. Phys. B*, 1996, **10**, 2577.
43 R. Morrish, Wiley, New York, 1966.
44 K. Wieghardt, K. Pohl, I. Jibril and G. Huttner, *Angew. Chem., Int. Ed. Engl.*, 1984, **23**, 77.
45 C. Delfs, D. Gatteschi, L. Pardi, R. Sessoli, K. Wieghardt and D. Hanke, *Inorg. Chem.*, 1993, **32**, 3099.
46 Y. Pontillon, A. Caneschi, D. Gatteschi, R. Sessoli, E. Ressouche, J. Schweizer and E. Lelievre-Berna, *J. Am. Chem. Soc.*, 1999, **121**, 5342.
47 R. Caciuffo, G. Amoretti, A. Murani, R. Sessoli, A. Caneschi and D. Gatteschi, *Phys. Rev. Lett.*, 1998, **81**, 4744.
48 I. Mirebeau, M. Hennion, H. Casalta, H. Andres, H. U. Gudel, A. V. Irodova and A. Caneschi, *Phys. Rev. Lett.*, 1999, **83**, 628.
49 J. R. Friedman, *Phys. Rev. B: Condens. Matter*, 1998, **57**, 10291.
50 C. Sangregorio, T. Ohm, C. Paulsen, R. Sessoli and D. Gatteschi, *Phys. Rev. Lett.*, 1997, **78**, 4645.
51 W. Wernsdorfer, T. Ohm, C. Sangregorio, R. Sessoli, D. Mailly and C. Paulsen, *Phys. Rev. Lett.*, 1999, **82**, 3903.
52 W. Wernsdorfer, A. Caneschi, D. Gatteschi, R. Sessoli, A. Villar and C. Paulsen, *Phys. Rev. Lett.*, in press.
53 W. Wernsdorfer and R. Sessoli, *Science*, 1999, **284**, 133.